Ultrathin and porous δ-FeOOH modified Ni_3S_2 3D heterostructure nanosheets with excellent alkaline overall water splitting performance

Xuefeng Ji[a,1], Chuanqi Cheng[b,1], Zehao Zang [a], Lanlan Li[a], Xiang Li[c], Yahui Cheng[d], Xiaojing Yang[a], Xiaofei Yu[a], Zunming Lu[a], Xinghua Zhang[a,], Hui Liu[b,*]*

X. F. Ji, Z. H. Zang, Prof L. L. Li, Prof X. J. Yang, Prof X. F. Yu, Prof Z. M. Lu, Prof X. H. Zhang
School of Materials Science and Engineering
Hebei University of Technology
Tianjin 300130, China
Email: zhangxinghua@hebut.edu.cn

C. Q. Cheng, Prof H. Liu
School of Materials Science and Engineering
Tianjin University
Tianjin 300072, China
Email: hui_liu@tju.edu.cn.

X. Li
Graduate School
Hebei University of Technology
Tianjin 300401, China

Prof Y. H. Cheng
Department of Electronics
Nankai University
Tianjin 300350, China

[*]Corresponding author. Tel.: +86 022 60204805, Email: zhangxinghua@hebut.edu.cn; hui_liu@tju.edu.cn.

Supporting Information

Calculation details:

For the construction of the heterojunction model, first we used Ni_3S_2 with a space group of R32 as the base and built a δ-FeOOH with a space group of P$\bar{3}$m1 on it. In order to ensure the stability of the heterjunction, we used the (110) crystal plane of Ni_3S_2 and the (100) crystal plane of δ-FeOOH to build it, and used a coexisting layer of S and O at the position where the two interfaces contacted to ensure a smooth transition. After this heterojunction is optimized and stabilized, we cut away half of the δ-FeOOH so that we get the place where the catalysis takes place.

All periodic slabs have a vacuum layer of at least 15 Å. In calculations, the one bottom Ni layers and S layers were fixed at their optimized bulk-truncated positions during geometry optimization, and the rest of atoms were allowed to relax. When the heterojunction was cut, one side of δ-FeOOH will be fixed to simulate the properties of the bulk. The size of the model after optimization is a = 12.38Å, b = 8.93Å, c = 39.79Å, α= β= γ=90°.

Adsorption free energy calculation.

The adsorption energy of reaction intermediates, can be computed using the following Equation (1):

$$\Delta G_{ads} = E_{ads} - E_{*} + \Delta E_{ZPE} - T\Delta S \tag{1}$$

Where ads = (OH^*, O^*, OOH^* or H^*), and ($E_{ads} - E_{*}$) is the binding energy, ΔE_{ZPE} is the zero-point energy change, ΔS is the entropy change. In this work, the values of ΔE_{ZPE} and ΔS were obtained by vibration frequency calculation.

The Gibbs free energy of the five reaction steps can be calculated by the following four Equations (2)-(6):

$$OH^- + {}^* \leftrightarrow HO^* + e^-$$

$$\Delta G_1 = \Delta G_{HO^*} - \Delta G_{*} - eU + k_b \ln a_{H^+} \tag{2}$$

$$HO^* + OH^- \leftrightarrow O^* + H_2O(l) + e^-$$

$$\Delta G_2 = \Delta G_{O^*} - \Delta G_{HO^*} - eU + k_b \ln a_{H^+} \tag{3}$$

$$O^* + OH^- \leftrightarrow HOO^* + e^-$$

$$\Delta G_3 = \Delta G_{OOH^*} - \Delta G_{O^*} - eU + k_b \ln a_{H^+} \tag{4}$$

$$OO^* + OH^- \leftrightarrow {}^* + O_2 + H_2O(l) + e^-$$

$$\Delta G_4 = \Delta G_{OO^*} - \Delta G_{O_2} - eU + k_b \ln a_{H^+} \tag{5}$$

$$H^+ + {}^* + e^- \leftrightarrow H^*$$

$$\Delta G_H = \Delta G_{H^*} - \Delta G_* - eU + k_b \ln a_{H^+} \tag{6}$$

In this work, $\Delta G_{1-4,H}$ were calculated at U=0 and pH=0.

Supporting results:

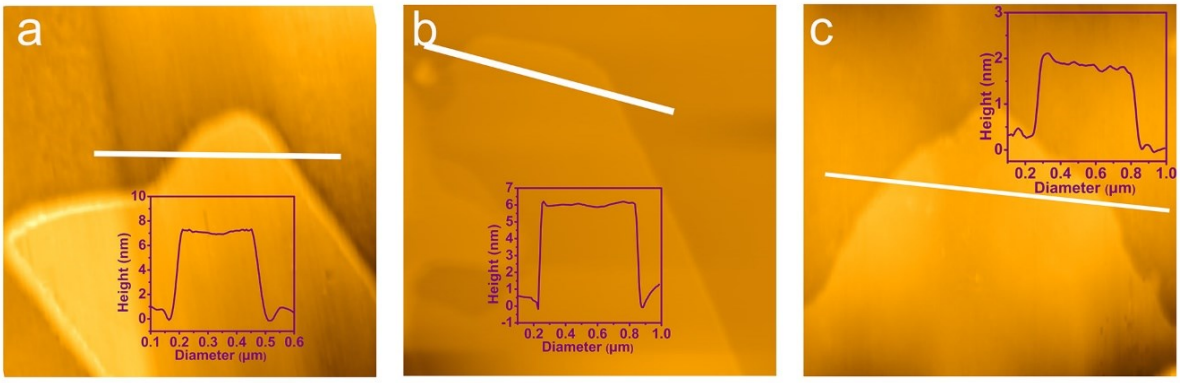

Figure S1. AFM images and corresponding line-scan profiles for a) δ-FeOOH/Ni_3S_2 nanosheets, b) Ni_3S_2 nanosheets, c) δ-FeOOH nanosheets, respectively.

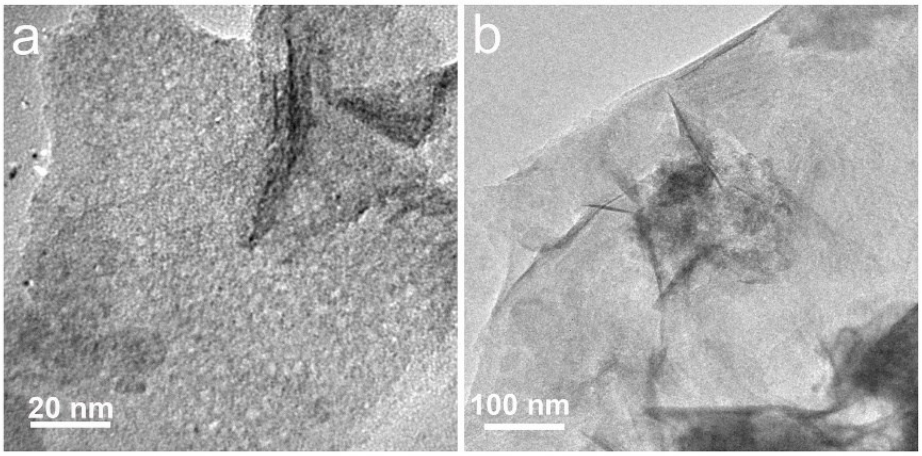

Figure S2. TEM images of a) δ-FeOOH nanosheets, and b) Ni_3S_2 nanosheets.

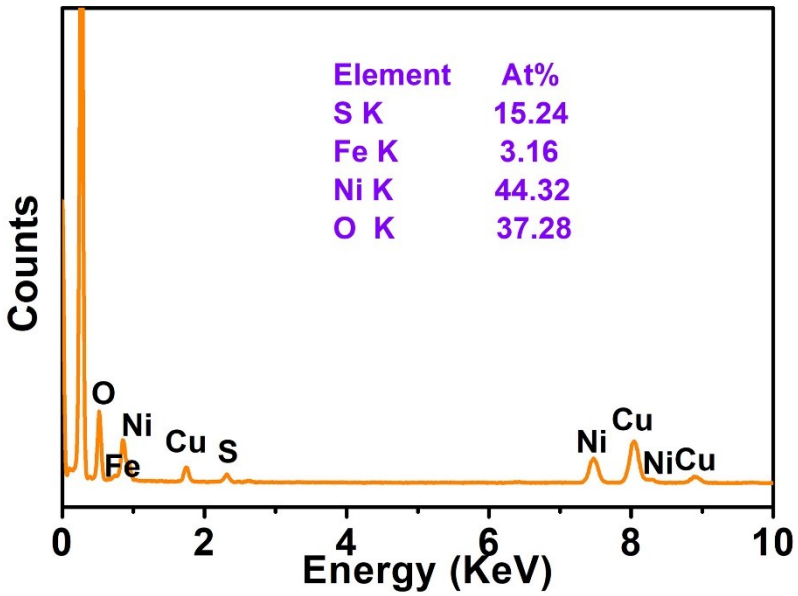

Figure S3. EDX spectrum of δ-FeOOH/Ni_3S_2 nanosheets with the corresponding elements ratio of Ni, Fe, O and S.

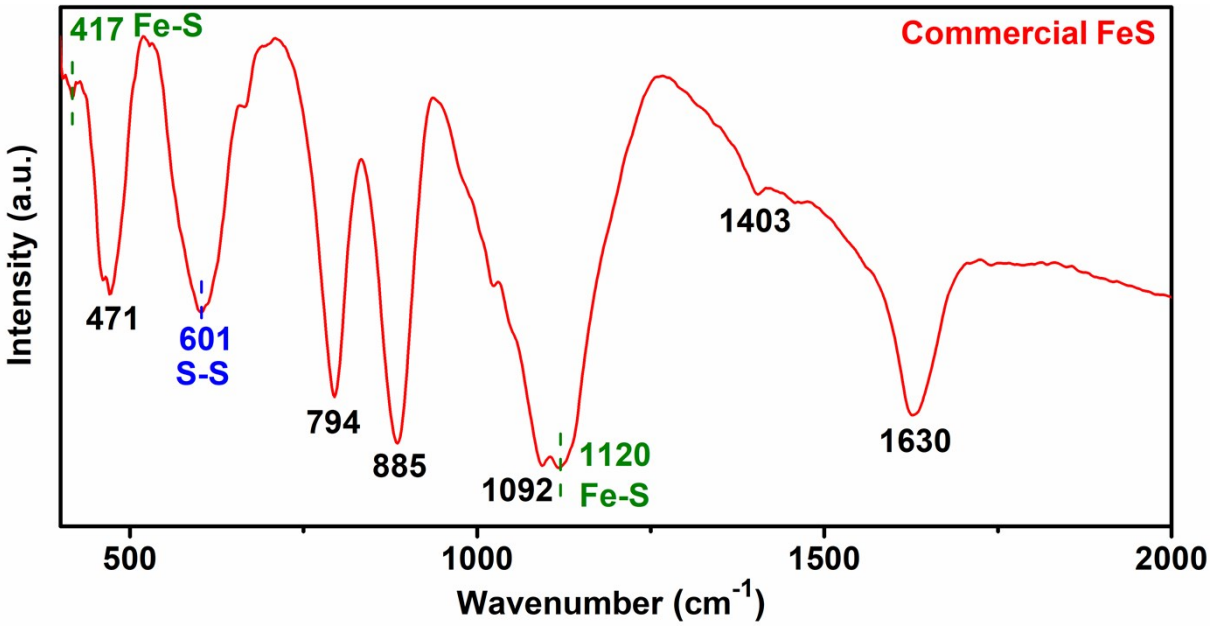

Figure S4. FTIR spectrum of commercial FeS and Fe-S bonds[1, 2].

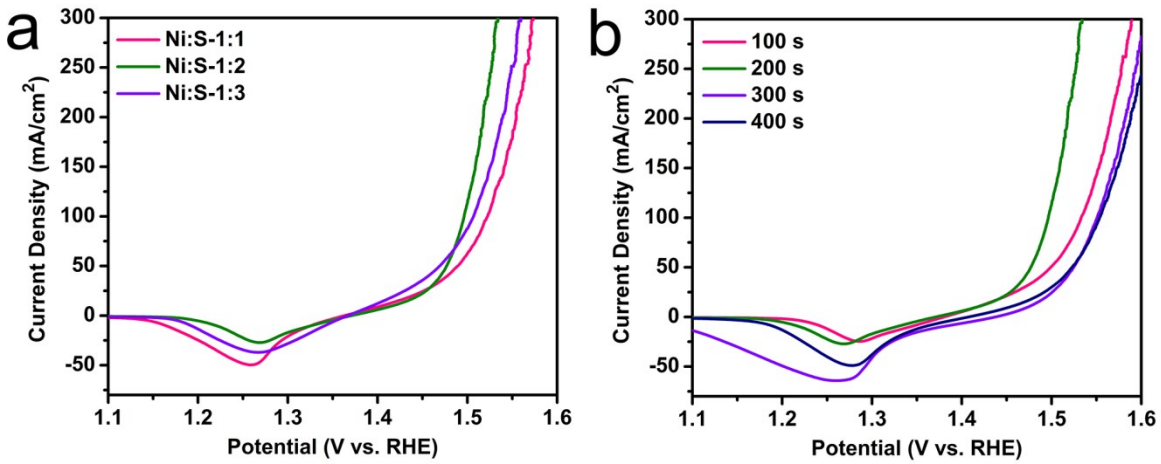

Figure S5. a) LSV polarization curves of OER for δ-FeOOH/Ni_3S_2/NF prepared with different Ni/S ratios; b) LSV polarization curves of OER for δ-FeOOH/Ni_3S_2/NF prepared with different δ-FeOOH deposition times.

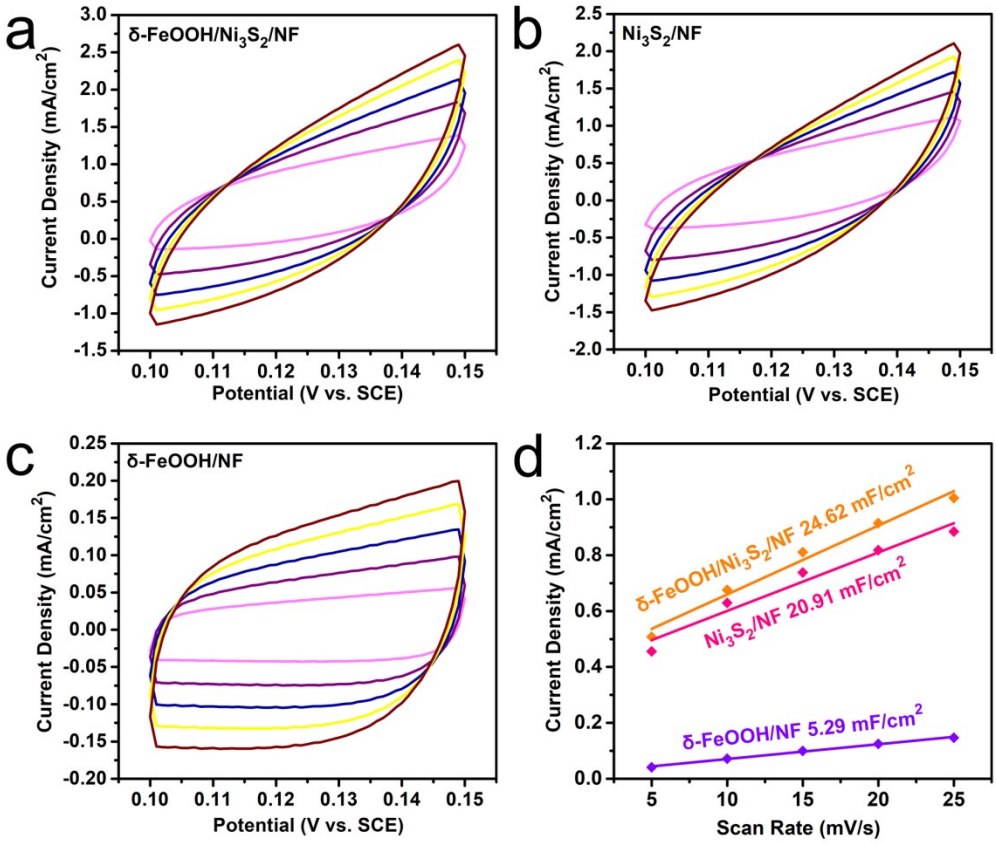

Figure S6. CV curves of a) δ-FeOOH/Ni_3S_2/NF, b) Ni_3S_2/NF and c) δ-FeOOH/NF for oxygen evolution obtained with scanning rate of 5 mV s^{-1}, 10 mV s^{-1}, 15 mV s^{-1}, 20 mV s^{-1} and 25 mV s^{-1}, respectively. d) Slope values C_{dl} of $\Delta J=(J_1-J_2)/2$ for all as-obtained catalysts plotted against scan rates, current density as a function of the scan rate for all as-obtained catalysts.

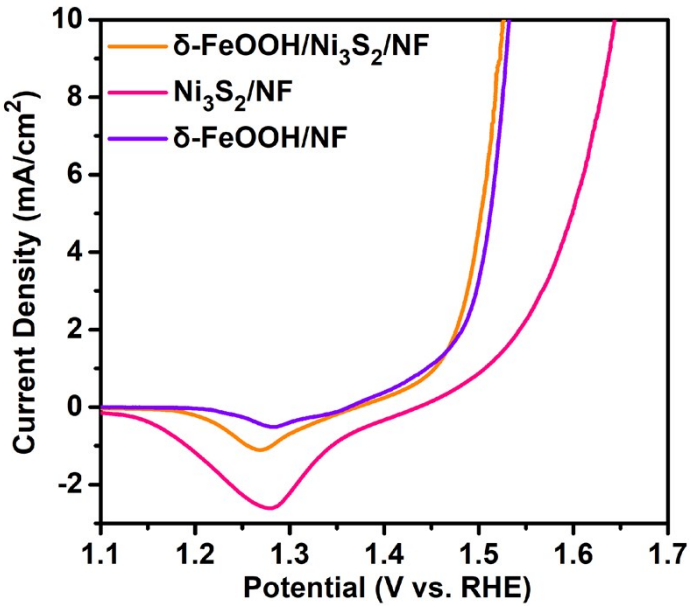

Figure S7. OER polarization curves of δ-FeOOH/Ni_3S_2/NF, Ni_3S_2/NF and δ-FeOOH/NF which are normalized into ECSA.

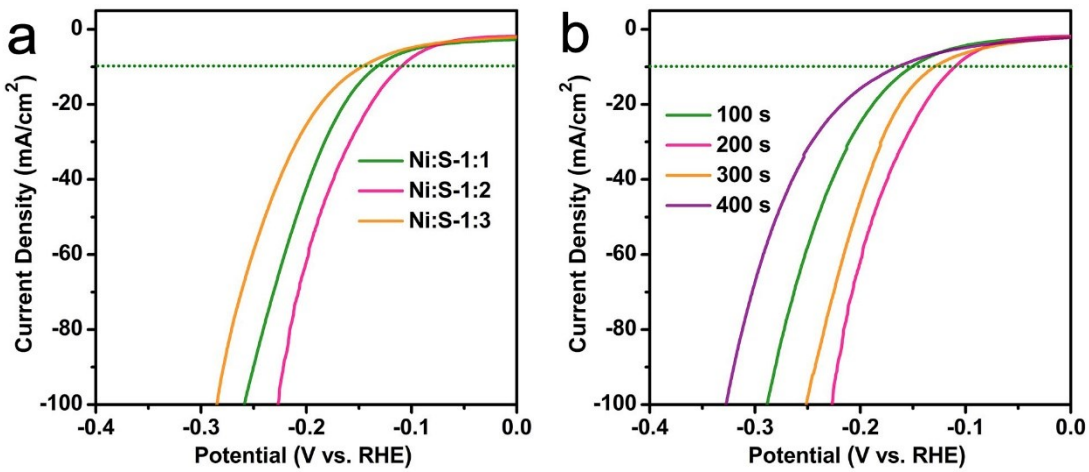

Figure S8. a) LSV polarization curves of HER for δ-FeOOH/Ni_3S_2/NF prepared with different Ni/S ratios; b) LSV polarization curves of HER for δ-FeOOH/Ni_3S_2/NF prepared with different δ-FeOOH deposition times.

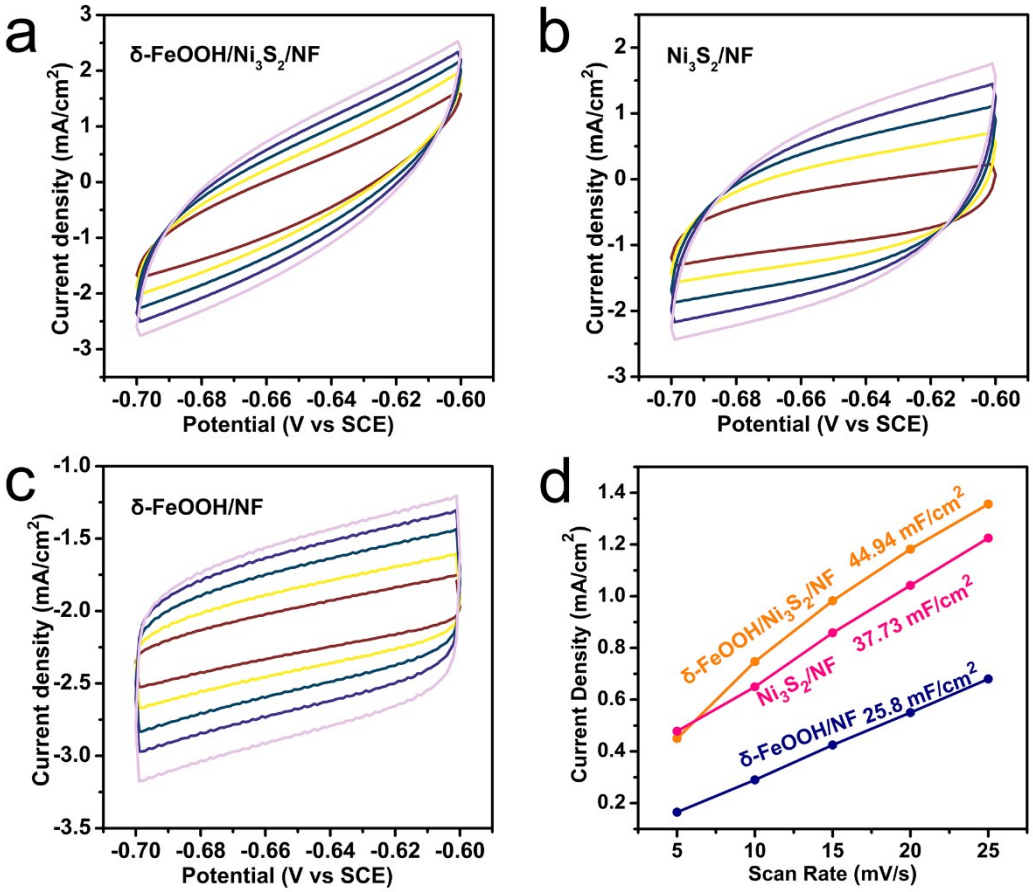

Figure S9. CV curves of a) δ-FeOOH/Ni_3S_2/NF, b) Ni_3S_2/NF and c) δ-FeOOH/NF for hydrogen evolution obtained with scanning rate of 5 mV s^{-1}, 10 mV s^{-1}, 15 mV s^{-1}, 20 mV s^{-1} and 25 mV s^{-1}, respectively. d) Slope values C_{dl} of $\Delta J=(J_1-J_2)/2$ of all as-obtained catalysts plotted against scan rates, current density as a function of the scan rate for all as-obtained catalysts.

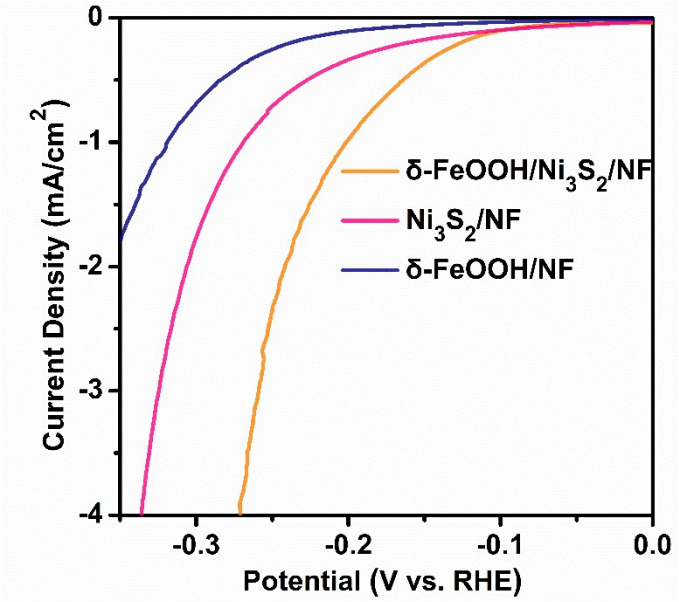

Figure S10. HER polarization curves of δ-FeOOH/Ni_3S_2/NF, Ni_3S_2/NF and δ-FeOOH/NF which are normalized into ECSA.

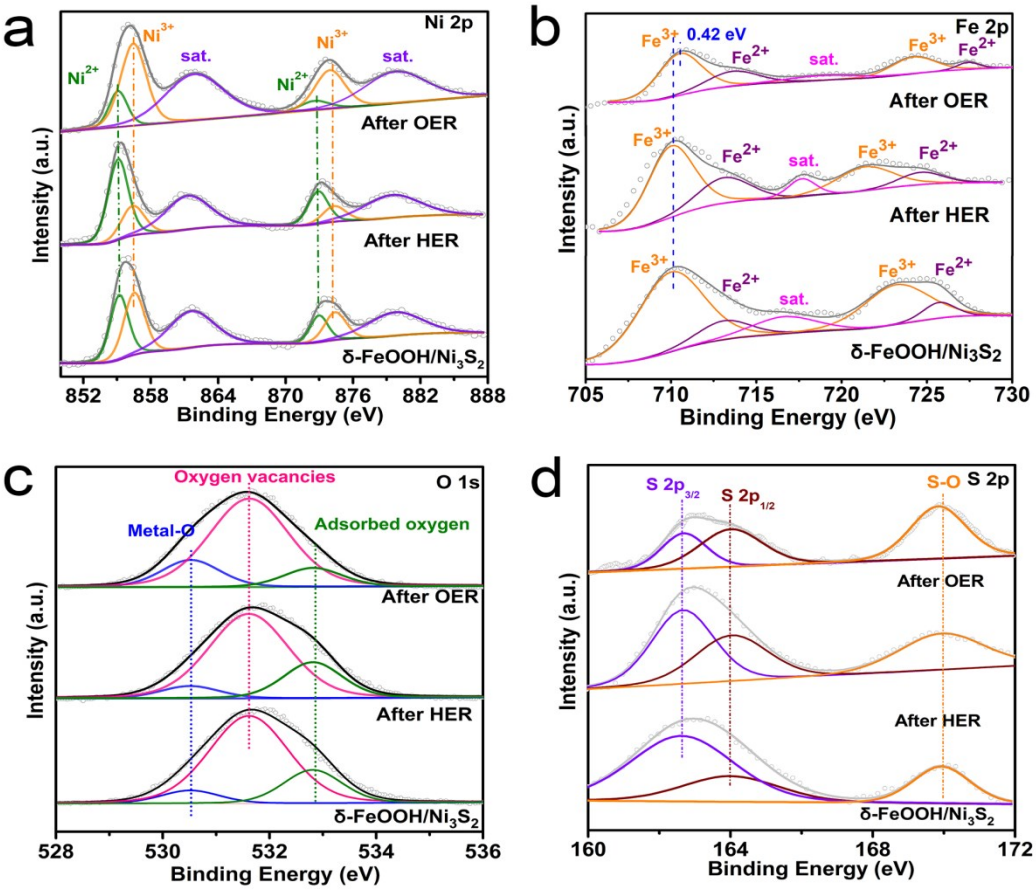

Figure S11. XPS spectra of δ-FeOOH/Ni_3S_2 after OER and HER testing for a) Ni 2p, b) Fe 2p, c) O 1s, and d) S 2p, respectively.

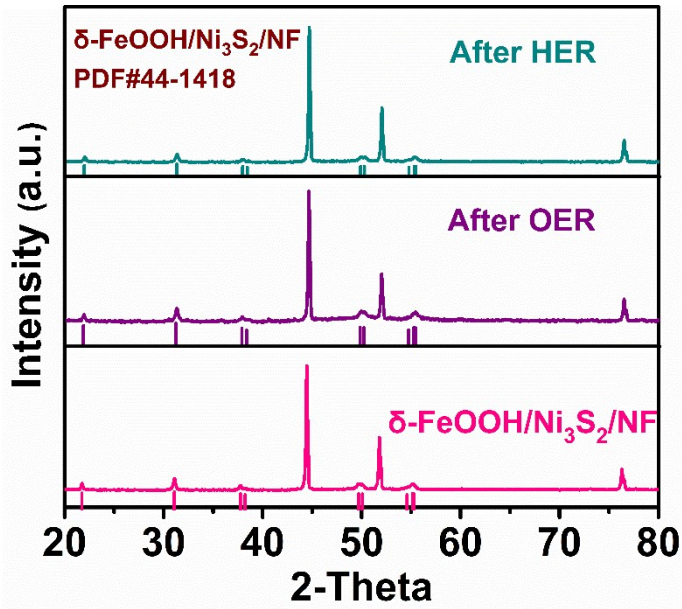

Figure S12. XRD patterns of δ-FeOOH/Ni_3S_2/NF before and after electrochemical test

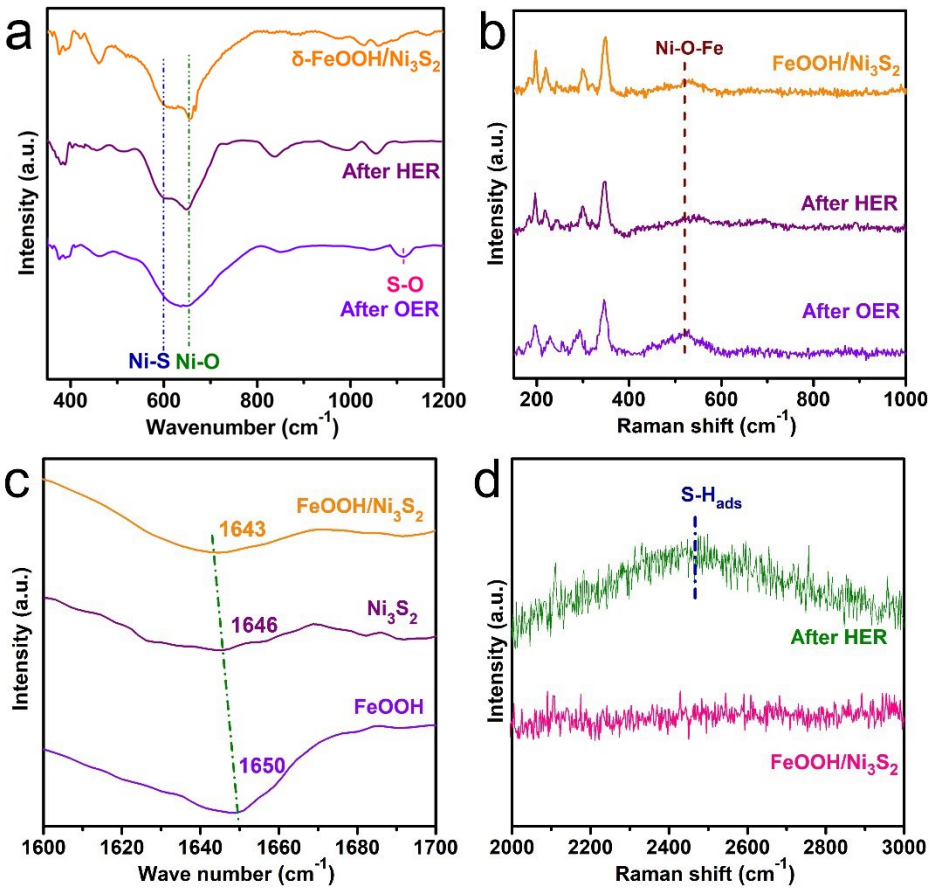

Figure S13. a) FTIR spectra and b) Raman spectra of δ-FeOOH/Ni_3S_2 after OER and HER testing, c) FTIR spectra of δ-FeOOH/Ni_3S_2, Ni_3S_2 and δ-FeOOH after HER testing, d) Raman spectra of δ-FeOOH/Ni_3S_2 after HER testing.

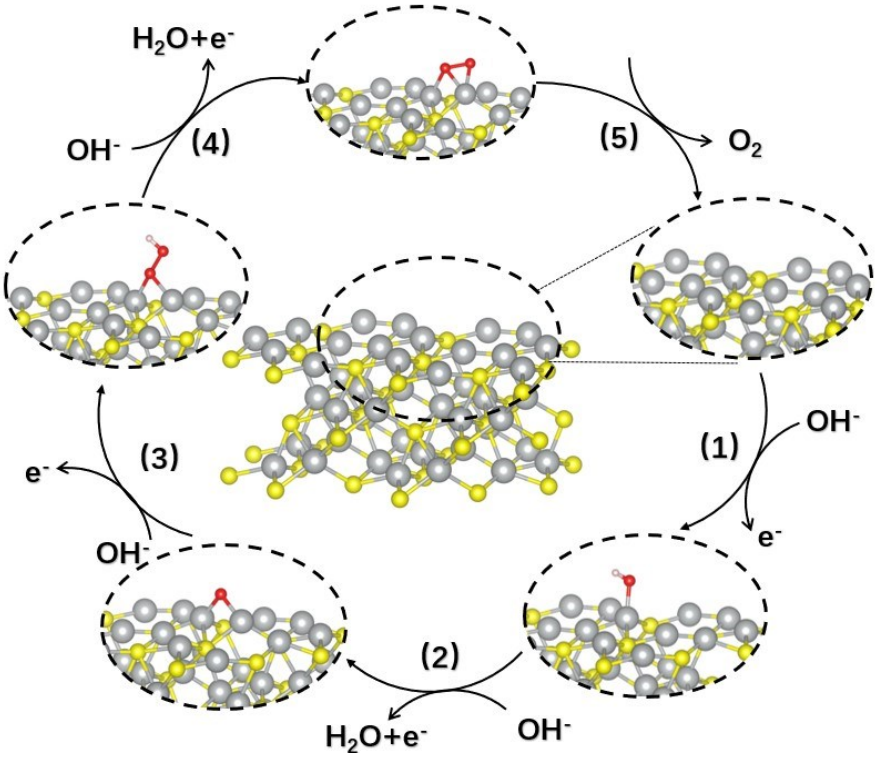

Figure S14. Structure model and schematic illustration of the OER pathway for Ni_3S_2.

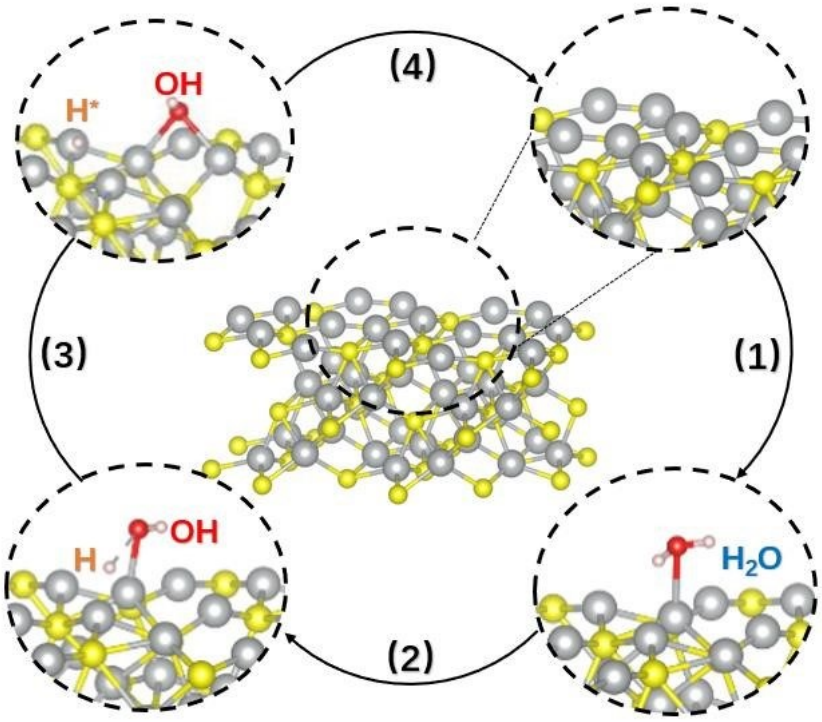

Figure S15. Structure model and schematic illustration of the dissociation of water pathway for Ni_3S_2 in HER process.

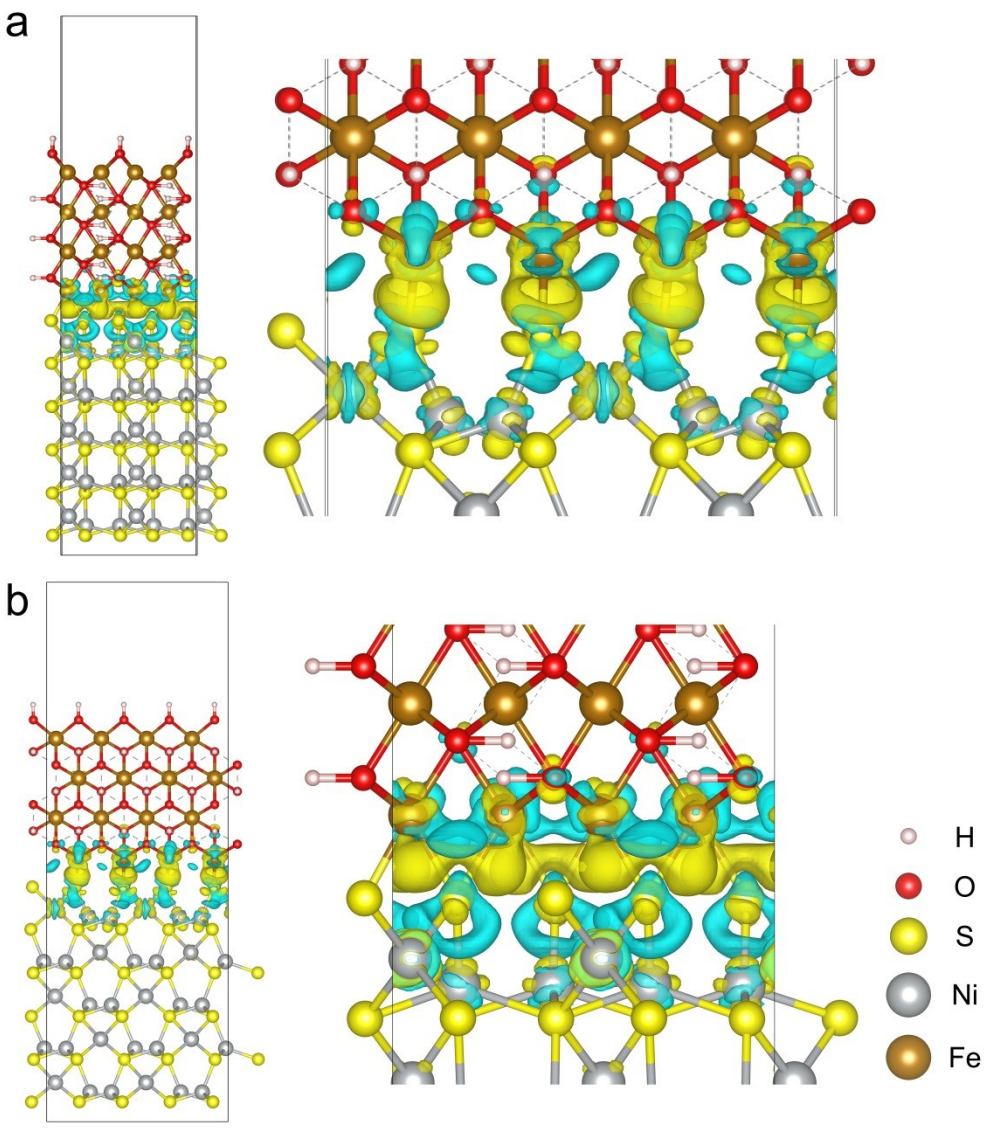

Figure S16. The Ni_3S_2(110) is used as substrate and FeOOH(100) is supported, the model is used to analyze the charge density difference at the interface, (a) front view, (b) side view. Yellow and blue indicate electron-rich and electron-deficient areas, and $3.5*10^{-3}$ *e* per $Bohr^3$ was used as the isosurface unit.

Table S1. Comparison of OER performance in alkaline media for δ-FeOOH/Ni_3S_2/NF and other OER electrocatalysts.

Catalyst	Electrolyte	ŋ (mV) @j (mA cm^{-2})	Electrode	References
δ-FeOOH/Ni_3S_2/NF	1.0 M KOH	187 mV @ 10 mA cm^{-2}	Ni foam	**This work**
$Fe_{0.33}Co_{0.67}OOH$ PNSAs	1.0 M KOH	266 mV @ 10 mA cm^{-2}	Carbon fiber cloth	[3]
FeOOH/Co/FeOOH HNTAs	1.0 M NaOH	250 mV @ 20 mA cm^{-2}	Ni foam	[4]
N-CoFe LDHs	1.0 M KOH	233 mV @ 10 mA cm^{-2}	Ni foam	[5]
h-NiFeCr	1.0 M KOH	220 mV @ 100 mA cm^{-2}	Ni foam	[6]
NiFe ANTAs	1.0 M KOH	220 mV @ 10 mA cm^{-2}	Carbon fiber cloth	[7]
CS-NiFeCu	1.0 M KOH	180 mV @ 10 mA cm^{-2}	Ni foam	[8]
$NiCeO_xH_y$	1.0 M KOH	177 mV @ 10 mA cm^{-2}	Graphite	[9]
FeS_2/CoS_2 NSs	1.0 M KOH	302 mV @ 100 mA cm^{-2}	Ni foam	[10]
Ni_3S_2	1.0 M KOH	242 mV @ 10 mA cm^{-2}	Ni foam	[11]
CoS_x/Ni_3S_2	1.0 M KOH	280 mV @ 20 mA cm^{-2}	Ni foam	[12]
$(Ni_{0.33}Co_{0.67})S_2$ NWs	1.0 M KOH	295 mV @ 100 mA cm^{-2}	Carbon fiber cloth	[13]

Table S2. Comparison of HER performance in alkaline media for δ-FeOOH/Ni_3S_2/NF and other HER electrocatalysts.

Catalyst	Electrolyte	ŋ (mV) @j (mA cm^{-2})	Electrode	References
δ-FeOOH/Ni_3S_2/NF	1.0 M KOH	106 mV @ 10 mA cm^{-2}	Ni foam	**This work**
NiP_2/NiO NRs	1.0 M KOH	131 mV @ 10 mA cm^{-2}	Carbon fiber paper	[14]
Ni/NiO NSs	1.0 M KOH	110 mV @ 5 mA cm^{-2}	Ni foam	[15]
$Ni(OH)_2$-CoS_2	1.0 M KOH	99 mV @ 20 mA cm^{-2}	Carbon fiber cloth	[16]
$MoS_2/Fe_5Ni_4S_8$	1.0 M KOH	120 mV @ 10 mA cm^{-2}	FeNi foam	[17]
MoS_2–Ni_3S_2 HNRs	1.0 M KOH	98 mV @ 10 mA cm^{-2}	Ni foam	[18]
$Co(S_{0.71}Se_{0.29})_2$	1.0 M KOH	122 mV @ 10 mA cm^{-2}	Ni foam	[19]
Co_9S_8@MoS_2	1.0 M KOH	143 mV @ 10 mA cm^{-2}	Ni foam	[20]

FeS_2/CoS_2 NSs	1.0 M KOH	78.2 mV @ 10 mA cm^{-2}	Ni foam	[10]
$(Ni_{0.33}Co_{0.67})S_2$ NWs	1.0 M KOH	334 mV @ 100 mA cm^{-2}	Carbon fiber cloth	[13]
$Fe_{0.1}$-NiS_2 NA	1.0 M KOH	250 mV @ 10 mA cm^{-2}	Ti mesh	[21]
NiFe LDH@NiCoP	1.0 M KOH	120 mV @ 10 mA cm^{-2}	Ni foam	[22]

Table S3. Comparison of overall water splitting performance in alkaline media for δ-FeOOH/Ni_3S_2/NF and other two-electrode devices.

Catalyst	**Electrolyte**	**ŋ (V) @j (mA cm^{-2})**	**Electrode**	**References**
δ-FeOOH/Ni_3S_2/NF	1.0 M KOH	1.525 V @ 10 mA cm^{-2}	Ni foam	**This work**
FeOOH	1.0 M KOH	1.62 V @ 10 mA cm^{-2}	Ni foam	[23]
$NiFe_2O_4$ NPs/NiFe LDH	1.0 M KOH	1.535 V @ 10 mA cm^{-2}	Ni foam	[24]
NiS	1.0 M KOH	1.64 V @ 10 mA cm^{-2}	Ni foam	[25]
Fe-Ni@NC-CNTs	1.0 M KOH	1.72 V@ 10 mA cm^{-2}	Ni foam	[26]
NiFe LDH/$NiCo_2O_4$	1.0 M KOH	1.60 V@ 10 mA cm^{-2}	Ni foam	[27]
$Co_{0.13}Ni_{0.87}Se_2$	1.0 M KOH	1.62 V@ 10 mA cm^{-2}	Ti mesh	[28]
Multishelled Ni_2P	1.0 M KOH	1.57 V@ 10 mA cm^{-2}	Carbon fiber paper	[29]
Ternary Ni-Fe-P Porous NRs	1.0 M KOH	1.52 V@ 10 mA cm^{-2}	Ni foam	[30]
NiFe LDH-NS@DG10	1.0 M KOH	1.5 V@ 20 mA cm^{-2}	Ni foam	[31]
$NiCo_2S_4$ NWs	1.0 M KOH	1.68 V@ 10 mA cm^{-2}	Ni foam	[32]
$Ni_{0.7}Fe_{0.3}S_2$	1.0 M KOH	1.625 V@ 10 mA cm^{-2}	Ni foam	[33]
3D Se-$(NiCo)S_x/(OH)_x$ Nanosheets	1.0 M KOH	1.60 V@ 10 mA cm^{-2}	Ni foam	[34]

References:

[1] F. T. Kong, X. H. Fan, A. G. Kong, Z. Q. Zhou, X. Y. Zhang, Y. K. Shan, *Adv. Funct. Mater.*, 2018, **28**, 1803973

[2] Z. Lei, F. Q. Dong, J. Liu, *Spectrochim. Acta A,* 2017, **173**, 544-548.

[3] S. H. Ye, Z. X. Shi, J. X. Feng, Y. X. Tong, G. R. Li, *Angew. Chem. Int. Ed.* 2018, **57**, 2672-2676.

[4] J. X. Feng, H. Xu, Y. T. Dong, S. H. Ye, Y. X. Tong, G. R. Li, *Angew. Chem. Int. Ed.* 2016, **55**, 3694-3698.

[5] Y. Y. Wang, C. Xie, Z. Y. Zhang, D. D. Liu, R. Chen, S. Y. Wang, *Adv. Funct. Mater*. 2018, **28**, 1703363.

[6] X. Bo, Y. B. Li, R. K. Hocking, C. Zhao, *ACS Appl. Mater. Inter.* 2017, **9**, 41239-41245.

[7] A. L. Wang, Y. T. Dong, M. Li, C. L. Liang, G. R. Li, *ACS Appl. Mater. Inter*. 2017, **9**, 34954-34960.

[8] P. L. Zhang, L. Li, D Nordlund, H. Chen, L. Z. Fan, B. B. Zhang, X. Sheng, Q. Daniel, L. C. Sun, *Nat. Commun.* 2018, **9**, 381.

[9] Z. H. Yan, H. M. Sun, X. Chen, H. H. Liu, Y. R. Zhao, H. X. Li, W. Xie, F. Y. Cheng, J. Chen, *Nat. Commun.* 2018, **9**, 2373.

[10] Y. X. Li, J. Yin, L. An, M. Lu, K. Sun, Y. Q. Zhao, D. Q. Gao, F. Y. Cheng, P. X. Xi, *Small* 2018, **14**, 1801070.

[11] J. F. Zhang, Y. Li, T. Y. Zhu, Y. Wang, J. W. Cui, J. J. Wu, H. Xu, X. Shu, Y. Q. Qin, H. M. Zheng, P. M. Ajayan, Y. Zhang, Y. C. Wu, *ACS Appl. Mater. Inter*. 2018, **10**, 31330-31339.

[12] S. Subhasis, S. Chhetri, W. Jang, N. C. Murmu, H. Koo, P. Samanta, T. Kuila, *ACS Appl. Mater. Inter*. 2018, **10**, 27712-27722.

[13] Q. Zhang, C. Ye, X. L. Li, Y. H. Deng, B. X. Tao, W. Xiao, L. J. Li, N. B. Li, H. Q. Luo, *ACS Appl. Mater. Inter*. 2018, **10**, 27723-27733.

[14] M. Y. Wu, P. F. Da, T. Zhang, J. Mao, H. Liu, T. Ling, *ACS Appl. Mater. Inter.* 2018, **10**, 17896-17902.

[15] X. D. Yan, L. H. Tiao, X. B. Chen, *J. Power Sources* 2015, **300**, 336-343.

[16] L. L. Chen, J.Y. Zhang, X. Ren, R. X. Ge, W. Q. Teng, X. P. Sun, X. M. Li, *Nanoscale* 2017, **9**, 16632-16637.

[17] Y. Wu, F. Li, W. L. Chen, Q. Xiang, Y. L. Ma, H. Zhu, P. Tao, C. Y. Song, W. Shang, T. Deng, J. B. Wu, *Adv. Mater.* 2018, **30**, 1803151.

[18] Y. Q. Yang, K. Zhang, H. L. Lin, X. Li, H. C. Chan, L. C. Yang, Q. S. Gao, *ACS Catal*. 2017, **7**, 2357-2366.

[19] L. Fang, W. X. Li, Y. X. Guan, Y. Y. Feng, H. J. Zhang, S. L. Wang, Y. Wang, *Adv. Funct. Mater.* 2018, **27**, 1701008.

[20] J. M. Bai, T. Meng, D. L. Guo, S. G. Wang, B. G. Mao, M. H. Cao, *ACS Appl. Mater. Inter*. 2018, **10**, 1678-1689.

[21] N. Yang, C. Tang, K. Wang, G. Du, A. M. Asiri, X. Sun, *Nano Res.* 2016, **9**, 3346-3354.

[22] H. J. Zhang, X. P. Li, A. Hähnel, V Naumann, C. Lin, S. Azimi, S. L. Schweizer, A. W. Maijenburg, R. B. Wehrspohn, *Adv. Funct. Mater.* 2018, **28**, 1706847.

[23] B. Liu, Y. Wang, H. Q. Peng, R. O. Yang, Z. Jiang, X. T. Zhou, C. S. Lee, H. J. Zhao, W. J. Zhang, *Adv. Mater*. 2018, **30**, 1803144.

[24] Z. C. Wu, Z. X. Zou, J. S. Huang, F. Gao, *ACS Appl. Mater. Inter*. 2018, **10**, 26283-26292.

[25] W. X. Zhu, X. Y. Yue, W. T. Zhang, S. X. Yu, Y. H. Zhang, J. Wang, J. L. Wang, *Chem. Commun*. 2016, **52**, 1486-1489.

[26] X. J. Zhao, P. Pachfule, S. Li, J. R. J. Simke, J. Schmidt, A. Thomas, *Angew. Chem. Int. Ed*. 2018, **57**, 8921-8926.

[27] Z. Q. Wang, S. Zeng, W. H. Liu, X. W. Wang, Q. W. Li, Z. G. Zhao, F. X. Geng, *ACS Appl. Mater. Inter*. 2017, **9**, 1488-1495.

[28] T. T. Liu, A. M. Asiri, X. P. Sun, *Nanoscale* 2016, **8**, 3911-3915.

[29] H. M. Sun, X. B. Xu, Z. H. Yan, X. Chen, F. Y. Cheng, P. S. Weiss, J. Chen, *Chem. Mater*. 2017, **29**, 8539-8547.

[30] S. H. Ahn, A. Manthiram, *J. Mater. Chem. A* 2017, **5**, 2496-2503.

[31] Y. Jia, L. Z. Zhang, G. P. Gao, H. Chen, B. Wang, J. Z. Zhou, M. T. Soo, M. Hong, X. C. Yan, G. R. Qian, J. Zou, A. J. Du, X. D. Yao, *Adv. Mater*. 2017, **29**, 1700017.

[32] A. Sivanantham, P. Ganesan, S. Shanmugam, *Adv. Funct. Mater*. 2016, *26,* 4661-4672.

[33] J. H. Yu, G. Z. Cheng, W. Luo, *J. Mater. Chem. A* 2017, **5**, 15838-15844.

[34] C. L. Hu, L. Zhang, Z. J. Zhao, A. Li, X. X. Chang, J. L. Gong, *Adv. Mater.* 2018, **30**, 1705538.